AGU PUBLICATIONS

Global Biogeochemical Cycles

RESEARCH ARTICLE
10.1002/2013GB004729

Key Points:
- Nitrate is mainly regenerated in spring sea ice
- Evolution in spring from new to regenerated sea ice primary production
- Sea ice alone is unlikely to explain δ^{15}N variation in Antarctic sediments

Supporting Information:
- Readme
- Auxiliary Materials
- Figure S1
- Figure S2
- Figure S3
- Figure S4
- Figure S5
- Figure S6
- Figure S7

Correspondence to:
F. Fripiat,
ffripiat@ulb.ac.be

Citation:
Fripiat, F., D. M. Sigman, S. E. Fawcett, P. A. Rafter, M. A. Weigand, and J.-L. Tison (2014), New insights into sea ice nitrogen biogeochemical dynamics from the nitrogen isotopes, *Global Biogeochem. Cycles, 28*, 115–130, doi:10.1002/2013GB004729.

Received 9 SEP 2013
Accepted 16 JAN 2014
Accepted article online 24 JAN 2014
Published online 25 FEB 2014

New insights into sea ice nitrogen biogeochemical dynamics from the nitrogen isotopes

F. Fripiat[1,2,3], D. M. Sigman[2], S. E. Fawcett[2], P. A. Rafter[2], M. A. Weigand[2], and J.-L. Tison[1]

[1]Department of Earth and Environmental Sciences, Université Libre de Bruxelles, Brussels, Belgium, [2]Department of Geosciences, Princeton University, Princeton, New Jersey, USA, [3]Now at Earth and System Sciences and Analytical and Environmental Chemistry, Vrije Universiteit Brussel, Brussels, Belgium

Abstract We report nitrogen (N) isotopic measurements of nitrate, total dissolved nitrogen, and particulate nitrogen from Antarctic pack ice in early and late spring. Salinity-normalized concentrations of total fixed N are approximately twofold higher than in seawater, indicating that sea ice exchanges fixed N with seawater after its formation. The production of low-δ^{15}N immobile organic matter by partial nitrate assimilation and the subsequent loss of high-δ^{15}N nitrate during brine convection lowers the δ^{15}N of total fixed N relative to the winter-supplied nitrate. The effect of incomplete nitrate consumption in sea ice is thus similar to that in the summertime surface ocean, but the degree of nitrate consumption is greater in ice, leading to a higher δ^{15}N for organic N (~3.9‰) than in the open Antarctic Zone (~0.6‰). Relative to previous findings of very high-δ^{15}N organic matter in sea ice (up to 41‰), this study indicates that it would be difficult for sea ice to explain the high δ^{15}N of ice age Antarctic sediments. The partitioning of N isotopes between particulate and dissolved forms of reduced N suggests that primary production evolved from new to regenerated production from early to late spring. Even though nitrate assimilation raises the δ^{15}N of nitrate, the δ^{15}N of sea ice nitrate is frequently lower than that of seawater, providing direct evidence that the regeneration of reduced N in the ice includes nitrification, with mass and isotopic balances suggesting that nitrification supplies a substantial fraction (up to ~70%) of nitrate assimilated within Antarctic spring sea ice.

1. Introduction

Sea ice is a semisolid matrix permeated by a network of channels and pores that are variably connected with underlying seawater. The brine-filled spaces are colonized by a sympagic community that is both taxonomically diverse and metabolically active [*Thomas and Dieckmann*, 2002; *Deming*, 2010]. During its incorporation into the ice, the microbial community is subjected to major changes in biogeochemical and physical environment (including fluctuations in temperature, salinity, O_2, light, pH, and nutrients). These conditions change further during both consolidation and melting of the sea ice [*Thomas et al.*, 2010]. Sea ice primary production has been estimated to account for up to 25% of the total primary production in sea ice-covered waters (including the highly productive marginal ice zone) [*Legendre et al.*, 1992; *Arrigo and Thomas*, 2004] and more than 50% in perennially ice-covered waters [*Gosselin et al.*, 1997]. A thorough evaluation of the processes driving the temporal and spatial distribution of sea ice primary production is crucial for determining the role of sea ice in global biogeochemical cycles and its impact on the marine sedimentary record.

Nitrogen (N) is a key constituent of life and one of the major nutrients required by all organisms. In the ocean, N exists in a variety of oxidation states and is involved in a complex web of microbially mediated transformations, either to obtain N to synthesize biomass or to extract energy for growth. Evidence exists that processes such as N assimilation, N remineralization, nitrification, and denitrification are active in the brine network [*Priscu et al.*, 1990; *Gleitz et al.*, 1995; *Thomas et al.*, 2001; *Rysgaard et al.*, 2008]. However, little information exists on the relative importance of these processes or their seasonal evolution. This is partly because sea ice is particularly poorly suited for estimating rates based on manipulative techniques such as tracer incubations. Analysis of the natural N isotopic composition (δ^{15}N) of the various fixed N pools in sea ice has the potential to yield rate estimates that integrate over meaningful time scales, without manipulation until the time of sampling (δ^{15}N, in permil versus atmospheric N_2, $= (((^{15}N/^{14}N)_{sample}/(^{15}N/^{14}N)_{atm} - 1) \times 1000)$).

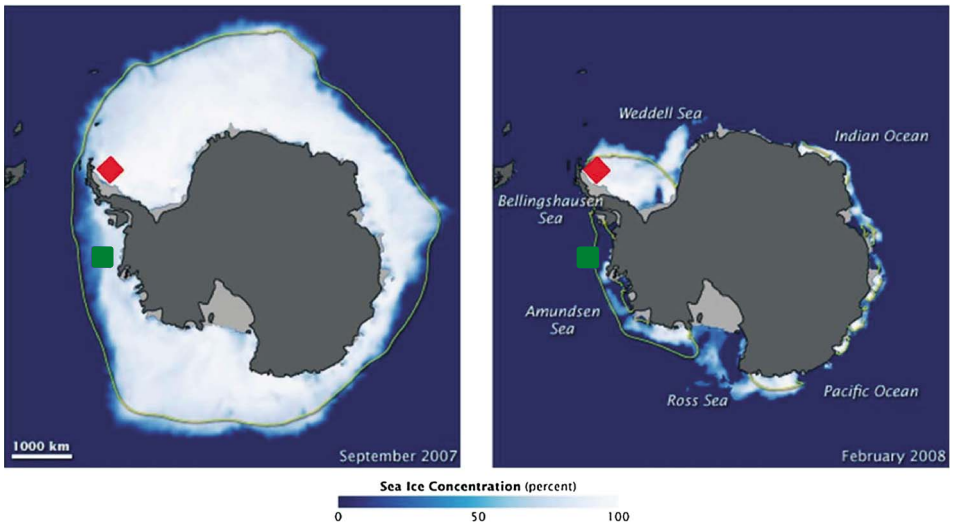

Figure 1. Satellite-based Antarctic sea ice extent in (left) September 2007 and (right) February 2008. The yellow line represents the median sea ice extent in September and February from 1979 to 2000. The red diamond is the ISPOL experiment (December 2004, ~68°S and 55°W) and the green square the SIMBA experiment (October 2007, ~70°S and 93°W). The pictures are taken from the NASA Earth Observatory website (http://earthobservatory.nasa.gov/Features/WorldOfChange/sea_ice_south.php).

Nitrogen transformations typically occur with measurable discrimination of the N isotopes. The degree of fractionation is given by the kinetic isotope effect, ε, defined by the ratio of rates at which the two isotopes are converted from one form to another (i.e., ε (‰) = $(({}^{14}k/{}^{15}k) - 1) \times 1000$); where ${}^{n}k$ is the rate coefficient for the ^{n}N-containing reactant [e.g., *Sigman et al.*, 1999]). For a given set of conditions, the mass and isotopic balances can be solved to quantify different N transformations.

The only study reporting the N isotopic composition of Antarctic sea ice observed a broad isotopic range for its particulate nitrogen (PN), 2 to 41‰ [*Rau et al.*, 1991], and the high values have been of particular interest. The ^{15}N:^{14}N of sinking biomass may provide a constraint on the ratio of nitrate uptake to gross nitrate supply in surface waters [*Altabet and François*, 1994]. ^{14}N-bearing nitrate is preferentially incorporated into organic N, leaving the residual nitrate pool enriched in ^{15}N [e.g., *Sigman et al.*, 1999]. As the initial nitrate supply is progressively consumed, the δ^{15}N of nitrate increases, leading to a related increase in the δ^{15}N of newly formed organic N. Antarctic sedimentary organic and diatom frustule-bound N from the last ice age is characterized by higher δ^{15}N than today, which has been interpreted as the result of more complete nitrate consumption in the surface waters of the ice age Antarctic [*François et al.*, 1997; *Robinson and Sigman*, 2008]. However, as an equatorward sea ice expansion is also expected during glacial periods [*Gersonde et al.*, 2005], the potentially higher contribution of sea ice PN in ice age sediments might contribute to or even entirely explain the observed ice age δ^{15}N elevation, nullifying the interpretation of an increase in the degree of nitrate consumption in the water column.

Here we report δ^{15}N measurements of nitrate (NO_3^-), total dissolved nitrogen (TDN), and particulate nitrogen (PN) at two Antarctic pack ice field sites, which we interpret as capturing two stages in the springtime evolution of pack ice. Significant variation was observed (a) with ice depth for a given N form, (b) among the different N forms, and (c) between the two field studies. We develop a mechanistic understanding of the processes driving sea ice N isotopic patterns, including the isotopic difference between sea ice and the water column. We show that brine convection, nitrate assimilation, organic N regeneration, and nitrification affect the partitioning of fixed N species (i.e., biologically available N) and their δ^{15}N. The implications for the δ^{15}N of sedimentary organic N in the Antarctic are also explored.

2. Site Description

Sea ice samples were collected at two drifting stations (Figure 1): ISPOL ("Ice Station POLarstern", 27 November 2004 to 2 January 2005, R/V *Polarstern*) in the Weddell Sea and SIMBA ("Sea Ice Mass Balance in

Antarctic", 24 September to 24 October 2007, R/V *Nathaniel B. Palmer*) in the Bellingshausen Sea. Both areas were characterized by first-year sea ice about 60 and 90 cm thick, with a thin snow cover (8–25 cm and 9–25 cm) and an overall positive freeboard (+1 to +3 cm and +1 to +5 cm) for SIMBA and ISPOL, respectively [*Tison et al*., 2008; *Lewis et al*., 2011]. All cores show the textural sequence typical of first-year sea ice: surface granular ice underlain by dominant columnar ice. Over the course of both the SIMBA and ISPOL experiments, basal melting of the ice floe was detected, of 5–15 cm and 9–15 cm, respectively [*McPhee*, 2008; *Lewis et al*., 2011].

Computed brine volume was always above the 5% threshold that indicates a permeable, interconnected brine network [*Cox and Weeks*, 1983; *Golden et al*., 1998; *Tison et al*., 2008; *Lewis et al*., 2011]. Computed brine salinity decreased with depth for both SIMBA and the first half of the ISPOL period [*Tison et al*., 2008; *Lewis et al*., 2011]. At sufficiently high permeability, the unstable vertical density gradient of the brine causes convection (so-called "gravity drainage"), which results in the exchange of brine with the underlying seawater [e.g., *Notz and Worster*, 2009]. At the end of ISPOL (from 14 to 31 December), brine salinity dropped below the seawater value due to ice melting, resulting in stratification of the brine network [*Tison et al*., 2008].

3. Materials and Methods

3.1. Sample Collection

Sampling occurred at least 1 km from the ship, using precautions to avoid organic matter contamination, which were also intended to be trace metal clean [e.g., *Lannuzel et al*., 2008]. Ice cores ($n = 9$) were collected at regular time intervals (approximately every week) in a selected area ($\approx 100\,m \times 100\,m$) of the ice floe, with each sampling corresponding to a square of $\approx 7.5\,m \times 7.5\,m$. Cores were collected using a 14 cm diameter electropolished stainless steel corer and were shipped back to the shore-based laboratory at −25°C in clean plastic bags in the dark. From each core, four ice blocks (≈15 cm thick) were cut at −25°C with a band saw ("prerinsed" by cutting a frozen block of 18 MΩ ultrapure deionized water). The external layer (≈ 1 cm) was removed with the same band saw before melting to prevent any contamination from sampling, manipulation, and storage.

Each ice block was sequentially melted at ambient temperature in the dark (four sequential fractions per ice block) [*Fripiat et al*., 2007], which enabled us to separate the different phases (brine versus pure ice) by their melting point. This method relies on the fact that the salty brine melts faster than the pure ice crystal matrix. Therefore, the interconnected brines (i.e., brine channels and feeder tubes) are drained first. To collect the closed structures (i.e., brine pockets), the surrounding pure ice must melt first, and they are therefore collected at the end (see Figure S1 in the supporting information for a discussion on the sequential melting approach and also Figure S2). The samples were immediately filtered through precombusted Whatman GF/F filters for SIMBA and prerinsed Nuclepore polycarbonate membranes (0.4 μm) for ISPOL. Filtered water samples were stored in 60 ml acid-washed, prerinsed polyethylene bottles at −25°C. Filters and membranes were also stored at −25°C. Bulk properties were computed using the weighted averages of the four sequential fractions. For the sake of clarity, the discussion will be primarily focused on bulk properties rather than the sequential fractions (see the supporting information, section 1, for the sequential fraction data and their interpretation).

3.2. Nitrogen Analyses

The concentration of nitrate plus nitrite ($[NO_3^-] + [NO_2^-]$) was measured by reduction to nitric oxide (NO) in a hot (95°C), acidic vanadium (III) solution, followed by chemiluminescence detection of NO [*Braman and Hendrix*, 1989] using a Teledyne 200E chemiluminescence NOx analyzer (Thousand Oaks, CA, U.S.). Nitrite concentration was measured by conversion to NO in a hot (95°C), acidic iodine solution, also followed by chemiluminescence detection [*Garside*, 1982]. The concentration of nitrate only was calculated by subtracting the measured concentration of nitrite only from that of nitrate plus nitrite. Ammonium concentration was measured using the fluorometric method of *Holmes et al*. [1999], but in only 21% of the samples because of limited sample volume.

Prior to nitrate isotope analysis, nitrite was removed via the sulfamic acid method of *Granger and Sigman* [2009]. The $\delta^{15}N$ of nitrate was analyzed by the "denitrifier method" [*Sigman et al*., 2001]. Briefly, 5–10 nmol of nitrate is quantitatively converted to N_2O gas by denitrifying bacteria that lack an active N_2O reductase. All of

the N atoms of nitrate are recovered as the N_2O gas analyte; the N isotopic composition is measured by gas chromatography/isotope ratio mass spectrometry (GC/IRMS, Thermo MAT253) with on-line cryotrapping. Measurements were referenced to air N_2 using the nitrate reference materials IAEA-N3, with a $\delta^{15}N$ of 4.7‰, and USGS-34, with a $\delta^{15}N$ of −1.8‰ [*Böhlke et al.*, 2003]. Seventy percent of our samples had a NO_3^- concentration lower than 3 μmol l^{-1}. For such concentrations (especially below 1 μmol l^{-1}), large volumes are required for the denitrifier method, and the highly variable salinities of our samples were a concern for precision. We developed a new evaporative technique to prepare such samples for nitrate $\delta^{15}N$ analysis at concentrations down to 0.25 μmol l^{-1} (see supporting information, section 2, for a description of this method). Replicate analyses (71% of the samples) indicate an average 1 standard deviation reproducibility of 0.14‰ (n = 102) for nitrate $\delta^{15}N$, including evaporated samples.

The concentration and $\delta^{15}N$ of total dissolved nitrogen (TDN = NO_3^- + NO_2^- + NH_4^+ + DON; DON being dissolved organic N) and particulate nitrogen (PN) were determined using the persulfate oxidation/denitrifier method of *Knapp et al.* [2005], which involves the oxidation of reduced fixed N species to nitrate, followed by the analysis of the concentration and $\delta^{15}N$ of the resultant nitrate using the chemiluminescence and denitrifier methods described above. To correct for the blank associated with the persulfate oxidizing reagent, triplicates of different amounts (15 and 60 nmol N) of two L-glutamic acid reference materials (USGS-40, with a $\delta^{15}N$ of −4.5‰, and USGS-41, with a $\delta^{15}N$ of 47.6‰) [*Qi et al.*, 2003] were processed along with the samples. Replicate analyses (43 and 84% of the samples) indicate an average 1 standard deviation reproducibility of 0.26 and 0.13‰ (n = 62 and 121) for TDN and PN $\delta^{15}N$, respectively. By measuring NO_3^- and TDN $\delta^{15}N$, we calculate the $\delta^{15}N$ of the remaining dissolved fixed nitrogen, which includes DON, NH_4^+, and NO_2^-.

4. Results

Similar to the salinity in sea ice brine, nutrient distribution in the brine changes because of temperature-induced dilution or concentration during melting and freezing processes. To correct for such effects, the nutrient concentrations were normalized to the salinity of underlying seawater (normalized concentration = SI concentration × SW salinity/SI salinity, where SI is sea ice and SW is seawater). As previously observed in spring/summer sea ice, most of samples exhibited an apparent NO_3^- depletion and DON + NH_4^+ accumulation relative to seawater (Figures 2a and 2c), driven by sea ice primary production (nitrate assimilation) and subsequent remineralization [e.g., *Gleitz et al.*, 1995; *Thomas et al.*, 2001].

For early spring measurements (SIMBA), NO_3^- concentration (normalized to seawater salinity) decreased from the bottom to the top of the ice, from 17.4 to 8.1 μmol l^{-1} (weighted averages for each depth; Figure 2a). A more severe NO_3^- depletion from 13.7 down to 1.7 μmol l^{-1} occurred in late spring (ISPOL; Figure 2c; especially at ~ 70% depth). NO_3^-, the major fixed N form in the underlying seawater, contributed only 22 ± 11% of the total fixed N within the ice. NO_2^- represented only a small fraction of NO_3^- + NO_2^- for SIMBA, but its contribution was greater at ISPOL (Figures 2a and 2c). The $\delta^{15}N$ of nitrate at SIMBA decreased toward the surface of the ice floe, from a weighted average of 5.1‰ at the sea ice bottom, similar to underlying seawater (5.0‰) [*Difiore et al.*, 2009], to an average of 4.1‰ at the top (Figure 2b). On average, the $\delta^{15}N$ of nitrate at ISPOL was higher than at SIMBA, but also decreased toward the surface, from 8.1‰ at the ice bottom to 4.0‰ at the surface (Figure 2d). We observed a minimum in the $\delta^{15}N$ of NO_3^- at the 70% depth at ISPOL (2.6‰), which corresponded with the lowest NO_3^- concentration.

For both SIMBA and IPSOL, a relatively constant DON + NH_4^+ + NO_2^- concentration (i.e., total dissolved nitrogen (TDN) minus NO_3^-; normalized to seawater salinity) was observed in the upper and internal levels of the ice (21 to 26 and 16 to 21 μmol l^{-1}, respectively, weighted averages for each depth; Figures 2a and 2c). The normalized DON + NH_4^+ + NO_2^- concentration was substantially higher at the ice bottom (39 and 59 μmol l^{-1} for SIMBA and ISPOL, respectively). NO_2^- and NH_4^+ represented 4 ± 3% and 20 ± 13% of this pool, respectively. Given the low NO_2^- contribution, hereafter this pool is referred to as DON + NH_4^+ only. Regardless of depth, TDN was dominated (76 ± 13%) by this DON + NH_4^+ pool, as is commonly reported in sea ice [e.g., *Thomas et al.*, 2001]. Using the NO_3^- and TDN $\delta^{15}N$, we infer the $\delta^{15}N$ of DON + NH_4^+. For both SIMBA and ISPOL, the $\delta^{15}N$ of DON + NH_4^+ showed a C-shaped depth profile: higher at the bottom and the surface of the ice and lower in the internal ice (Figures 2b and 2d). For ISPOL, the $\delta^{15}N$ of DON + NH_4^+ was on average higher than at SIMBA (0 to 2.5‰ and −2.4 to 1.3‰, respectively, weighted averages for each depth).

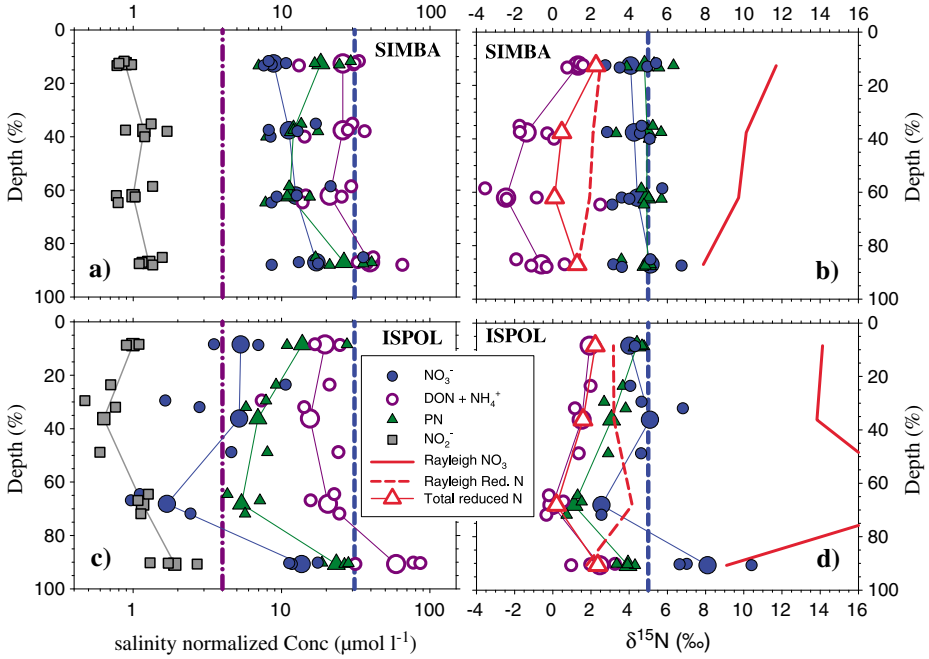

Figure 2. Salinity normalized concentrations of NO_3^- (blue circles), DON + NH_4^+ (purple open circles), PN (green triangles), and NO_2^- (gray squares) as a function of depth for (a) SIMBA and (c) ISPOL (depth % = middepth of the ice sample block/total ice thickness × 100; total thickness of approximately 60 and 90 cm for SIMBA and ISPOL, respectively). (b and d) The $\delta^{15}N$ of NO_3^- (blue circles), DON + NH_4^+ (purple open circles), PN (green triangles), and total reduced nitrogen (red open triangles; PN + DON + NH_4^+) as a function of depth (depth %), for SIMBA and ISPOL, respectively. Each small symbol corresponds to a weighted bulk measurement (i.e., an entire ice block), and the larger connected symbols are the weighted averages for each major depth interval. Seawater nitrate is indicated by the blue dashed lines and seawater DON by the purple dash-dotted lines. Red solid and dashed lines are, respectively, the computed nitrate $\delta^{15}N$ (equation (1)) and accumulated product $\delta^{15}N$ (equation (3)), assuming Rayleigh fractionation kinetics, an isotope effect of 5‰, and initial substrate equals to the seawater nitrate values shown.

For both SIMBA and ISPOL, the normalized PN concentration exhibited a C-shaped profile (with weighted averages for each depth of 5 to 23 and 11 to 26 µmol l^{-1}, respectively; Figures 2a and 2c). PN represented 28 ± 11% of the total fixed nitrogen (TN = TDN + PN). Its $\delta^{15}N$ was remarkably invariant with depth during SIMBA (4.8 to 5.0‰, Figure 2b), whereas at ISPOL, the $\delta^{15}N$ of PN presented a C-shaped vertical profile and was on average lower than at SIMBA (with weighted averages for each depth of 1.1 to 4.4‰, Figure 2d).

Both at SIMBA (16 October) and ISPOL (9 December), two profiles appear as "outliers" from the general trends. These profiles correspond to specific short-term events in brine dynamics [*Tison et al.*, 2008; *Lewis et al.*, 2011] that have an apparently marked effect on the N isotopic signatures. The profiles have therefore been removed from the weighted average calculations of both concentration and N isotopic composition, and they are discussed in the supporting information (section S3). For the 9 December ISPOL profile, seawater flooding over the top of the sea ice likely resulted in a new input of NO_3^- to the ice surface, an explanation that is supported by brine/ice $\delta^{18}O$ data [*Tison et al.*, 2008] (see section 5.1).

5. Discussion

Two sets of questions underlie this study of N isotope dynamics in Antarctic sea ice. First, what processes are driving the N isotopic balance, and what are the implications for our understanding of sea ice biogeochemical dynamics? Second, what are the potential impacts of sea ice N transformations on the N isotope dynamics of the upper ocean as a whole and, in turn, on Antarctic sedimentary $\delta^{15}N$? We address these in turn below.

5.1. Sea Ice Nitrogen Budget

In the Polar Antarctic Zone, deep mixing during the winter results in 31 µmol l^{-1} NO_3^- + NO_2^- at the surface, with a $\delta^{15}N$ of ~5.0‰ [*DiFiore et al.*, 2009; *Rafter et al.*, 2013]. While there are only minor amounts of ammonium in the winter mixed layer, the concentration of DON is poorly known in the wintertime Antarctic, and

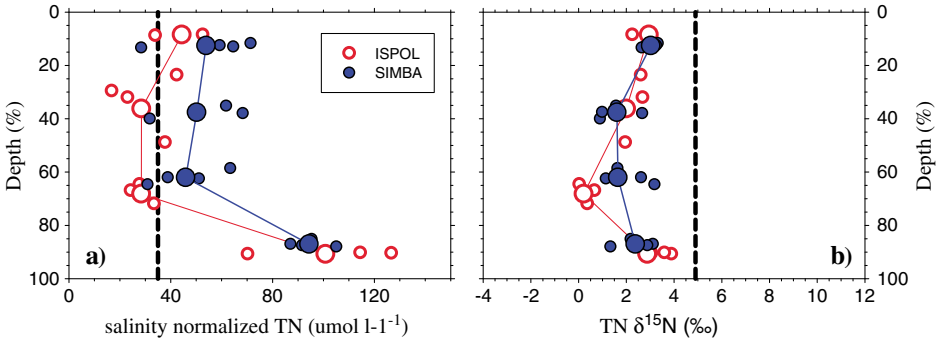

Figure 3. Salinity normalized concentration of total fixed nitrogen (a) and its δ^{15}N (b) in the ice as a function of depth (as in Figure 2). SIMBA is shown in filled blue circles and ISPOL in open red circles. Each small circle corresponds to a weighted bulk measurement, and the larger connected circles indicate the weighted averages for each depth interval. The estimated seawater total fixed nitrogen is indicated by the black dashed line.

the δ^{15}N of DON is only known for regions of the subtropical/tropical ocean. Assuming a concentration of $4.2 \pm 1.3\ \mu mol\ l^{-1}$ (mean in *Ogawa et al.* [1999] Southern Ocean in summer) and a δ^{15}N of 4‰ for DON [*Knapp et al.*, 2011] (subtropical/tropical ocean; range of 1 to 6‰), we calculate a wintertime seawater total fixed N (TN) concentration and δ^{15}N of 35 $\mu mol\ l^{-1}$ and 4.9‰, respectively. By considering the full range of previously measured DON δ^{15}N, TN δ^{15}N ranges from 4.5 to 5.1‰. The measured sea ice TN δ^{15}N was lower (0.0 to 3.9‰) than that of seawater (Figure 3b); this requires that ^{15}N is preferentially lost from sea ice.

Sea ice is a mixture of solid freshwater ice and liquid salty brine. When cooling occurs from above, as in the case of growing sea ice, the temperature profile, with temperature increasing downward, results in higher salinity brine above lower salinity brine. This generates an unstable vertical density gradient that has the potential to drive brine convection [*Notz and Worster*, 2009]. Theoretical considerations and model simulations strongly suggest that brine convection in first-year growing sea ice (~ in winter) only occurs very close to the ice-ocean interface (Figure 4), where most of the brine loss from sea ice occurs [*Griewank and Notz*, 2013]. This is related to the fact that convectional brine loss from sea ice only occurs when a sufficiently unstable vertical density gradient of the brine coincides with a sufficiently high permeability in the ice [*Notz and Worster*, 2009]. Whenever both of these conditions are met, brine is replaced by convective exchange with underlying sea water. Some of the intruding sea water will freeze within the sea ice, because the seawater is less salty than the brine it replaces. This then lowers permeability, and convection ceases. Episodic full-depth convection within sea ice will only set in once the ice has warmed sufficiently in the spring to increase permeability throughout the entire ice thickness (Figure 4) [*Jardon et al.*, 2013; *Griewank and Notz*, 2013]. Nitrogen can then be exchanged between sea ice and seawater. Any process that preferentially accumulates ^{15}N in the exchangeable (i.e., dissolved) N pools and traps ^{14}N in immobile pools within the ice is a viable explanation for the observed shift toward lower sea ice TN δ^{15}N.

Field-based estimates of the isotope effect for nitrate assimilation range from 4‰ to 10‰, with most estimates closer to 5–8‰ [e.g., *Difiore et al.*, 2010]. If nitrate assimilation is occurring, the residual nitrate pool is left enriched in ^{15}N. ^{14}N is preferentially incorporated into organic N, which is trapped within sea ice [*Meiners et al.*, 2004; *Deming*, 2010]. Brine convection expels residual nitrate with a high δ^{15}N out of the sea ice and replenishes it with seawater TN (predominantly nitrate) that is lower in δ^{15}N (Figure 4b). Associated with the initial building of biomass in spring, fueled by nitrate assimilation, this process should progressively deplete the total fixed N of ^{15}N, as observed throughout the ice floe (Figures 3b and 4). Such a mechanism is also consistent with the observation that the normalized TN concentration in the ice is generally higher than in seawater, implying an additional source of N to the ice (i.e., replenishment with seawater nitrate; Figure 3a). A potential weakness in this scenario is that the low-δ^{15}N DON + NH_4 pool should also be able to exchange with seawater (Figure 2). Given that DON + NH_4^+ is the largest N pool in the ice, brine convection should expel low-δ^{15}N DON + NH_4^+ out of sea ice, counterbalancing the effect of nitrate assimilation. To decrease TN δ^{15}N (from ~4.9 to ~2.2‰; Figure 3b), a fraction of the DON + NH_4^+ pool must remain trapped within sea ice. Indeed, laboratory studies indicate that dissolved organic matter produced by phytoplankton has a chemical affinity for sea ice [*Müller et al.*, 2013] (Figure 4b). This pool likely includes a significant fraction of colloidal organic matter (1–1000 nm) [*Verdugo et al.*, 2004] such as nanogel and microgel that stick to ice walls, or macrogels such as transparent exopolymeric particles, which are observed in abundance in sea ice [e.g., *Meiners et al.*, 2004].

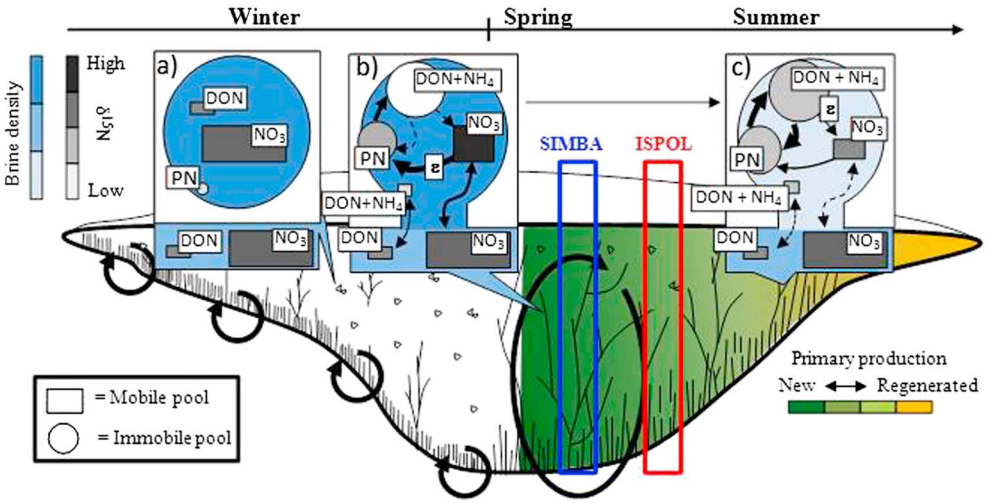

Figure 4. Conceptual scheme showing sea ice growth and decay and the associated nitrogen biogeochemical dynamics. (a–c) The large circles illustrate brine inclusions that are connected as shown in Figures 4b and 4c or disconnected as shown in Figure 4a from the seawater below. Color fillings represent relative intensities of chosen variables of interest: The relative density of the brine and seawater is given by the blue color bar, the relative $\delta^{15}N$ by the gray color bar, and the new versus regenerated primary production by the green-yellow color bar. The N pools are indicated within the brine inclusions, with their grayscale shade increasing with their $\delta^{15}N$ and their shape indicating whether they are mobile. The arrows among the N pools reflect biological fluxes (single sided) or exchanges (double sided), with thicker arrows qualitatively indicating greater fluxes and an "epsilon" label indicating that the isotopic observations are particularly affected by isotope fractionation at the labeled step. In winter when the ice is growing (Figure 4a), brine convection is observed only at the interface with the ocean where sea ice is permeable. At the surface and in the interior ice, the porosity is too low to allow convection, despite the high brine density. These brine structures are closed, with little or no biological activity. The brine composition is mainly inherited from the underlying seawater. At the beginning of spring (Figure 4b), both primary production and porosity increase, allowing nitrate assimilation (~ new primary production) into immobile organic matter and brine convection through the full thickness of the ice (due to brine density greater than seawater). ^{14}N is preferentially assimilated into organic matter, leaving the residual nitrate pool enriched in ^{15}N, which can then be exchanged with seawater through brine convection. This process decreases the total fixed nitrogen $\delta^{15}N$, as observed (Figure 3b). To match the observations (low TN $\delta^{15}N$), a significant fraction of the dissolved organic N (largest and lowest $\delta^{15}N$ pool) must remain trapped within the ice (circles in Figure 4b and 4c and discussion in the text). The $\delta^{15}N$ of $DON + NH_4^+$ is lower than PN, due to a net transfer of N from PN to $DON + NH_4^+$, with fractionation in the conversion. With the subsequent development of a biological community that regenerates and recycles N (Figure 4c; ~ regenerated primary production), including nitrifiers, N is mainly regenerated through the regeneration loop (PN, $DON \rightarrow NH_4 \rightarrow PN$), yielding a convergence between PN and $DON + NH_4^+$ $\delta^{15}N$, and a smaller fraction is regenerated back to nitrate through nitrification, decreasing nitrate $\delta^{15}N$. During the ice decay, a stratification inside the brine network is expected due to melting of the brine walls, limiting exchange to diffusion processes only (i.e., brine density lower than seawater [*Tison et al.*, 2008]).

It has been suggested that around much of Antarctica, when the snowpack is sufficiently thick to depress the ice surface below the sea level, seawater can infiltrate the ice, supplying nutrients to the ice surface [e.g., *Maksym and Markus*, 2008]. In our data set, the first occurrence of snow ice is observed in the 9 December ISPOL profile (discussed in section 3 of the supporting information), as it bears the characteristically lower $\delta^{18}O$ derived from the freezing of a mixture of meteoric ice, seawater, and brine [*Tison et al.*, 2008]. Further downward, infiltration of seawater into the underlying brine network is suggested from brine/ice $\delta^{18}O$ along the same profile [*Tison et al.*, 2008]. As with brine convection, flooding and subsequent downward infiltration would supply relatively lower seawater NO_3^- $\delta^{15}N$ to the brine network, washing the residual high-$\delta^{15}N$ NO_3^- downward into the underlying brine network. The higher NO_3^- concentration at all depths in the 9 December ISPOL profile, together with a TN $\delta^{15}N$ closer to the seawater end-member, is consistent with seawater flooding and infiltration (Figures S5 and S6).

5.2. Sea Ice Nitrogen Internal Cycling

The partitioning of fixed N among its various chemical species is dramatically different in sea ice than in Antarctic seawater, in which nitrate is the dominant N form. Near-complete nitrate assimilation and the concomitant accumulation of large algal standing stocks lead to a much larger contribution from organic N within sea ice (82 ± 9% of TN). If assimilation proceeds with a constant isotope effect (ε_{Nau}, NaU being nitrate

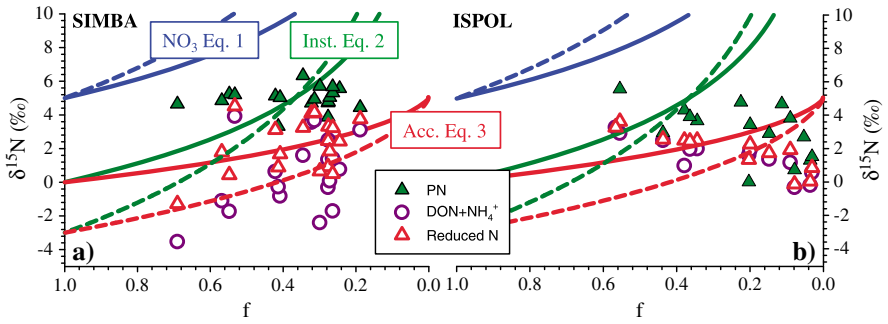

Figure 5. The δ^{15}N of the reactant (equation (1), blue lines), instantaneous product (equation (2), green lines), and accumulated product (equation (3), red lines) as per the Rayleigh fractionation model as a function of the fraction of the initial reactant (nitrate) pool that remains unconsumed (f, $[NO_3^-]/[NO_3^-]_{sw}$). The initial δ^{15}N and concentration of the reactant pool are based on the winter mixed layer seawater, and two different isotope effects for nitrate assimilation are considered, 5‰ (solid lines) and 8‰ (dashed lines). (a) SIMBA and (b) ISPOL for the δ^{15}N of PN (filled green triangles), DON + NH_4^+ (open purple circles), and of reduced N (PN + DON + NH_4^+; open red triangles).

assimilation, the U referring to uptake) and if the reactant (nitrate) and product (organic matter) N pools are neither replenished nor lost from the system, then the isotopic evolution of the residual nitrate, instantaneous PN (hereafter referred to with the superscript "inst"), and accumulated PN (hereafter referred to with the superscript "acc") would be described by Rayleigh fractionation kinetics (curves in Figure 5), with the following equations:

$$\delta^{15}N_{NO_3^-} = \delta^{15}N_{NO_3^- - SW} - \varepsilon_{NaU} \cdot \ln(f) \quad (1)$$

$$\delta^{15}N_{PN}^{inst} = \delta^{15}N_{NO_3^-} - \varepsilon_{NaU} \quad (2)$$

$$\delta^{15}N_{PN}^{Acc} = \delta^{15}N_{NO_3^- - SW} + \varepsilon_{NaU} \cdot \frac{f \cdot \ln(f)}{(1-f)} \quad (3)$$

where f is the fraction of residual nitrate;

$$f = \frac{NO_3^-}{NO_{3-SW}^-} \quad (4)$$

Not surprisingly for nitrate, our isotopic measurements are poorly described by these equations (Figure 2). Nitrate depletion increased upward through the ice, but the δ^{15}N of nitrate decreased toward the top. Furthermore, most of the samples (55%) had nitrate with a δ^{15}N lower than that of the underlying seawater (~5.0‰) [*Difiore et al.*, 2009]. If nitrate assimilation was the only process at work, nitrate δ^{15}N would have always been higher than that of seawater and should increase upward (Figures 2b and 2d). Another process must therefore be involved in the partitioning of the nitrate isotopes in the ice. Four processes can affect the δ^{15}N of nitrate: (i) nitrate assimilation, (ii) nitrification, (iii) denitrification, and (iv) N_2 fixation when coupled to N cycling and nitrification. Since both nitrate assimilation and denitrification preferentially consume ^{14}N, increasing the δ^{15}N of the residual nitrate, only nitrification and N_2 fixation are able to decrease the δ^{15}N of nitrate. While unexplored, N_2 fixation within sea ice is unlikely to occur at rates comparable to nitrate assimilation and the internal N cycling processes [e.g., *Thomas et al.*, 2010]. As we discuss in section 5.3. below, nitrification appears to explain the distribution of the N isotopes in sea ice, through the production of low-δ^{15}N nitrate. The coupling of low NO_3^- concentration and low δ^{15}N at the 70% depth of ISPOL suggest that higher degrees of NO_3^- depletion allow for the greatest isotopic imprint of nitrification (Figures 2c and 2d). This is to be expected, as a given quantity of NO_3^- produced from nitrification will represent a greater fraction of the total NO_3^- when the background [NO_3^-] is low.

For SIMBA, we observe PN with a δ^{15}N that is higher than the Rayleigh fractionation prediction for the accumulated product of nitrate assimilation (equation (3) and Figure 2b). This can be explained by isotopic discrimination during the conversion of PN into DON + NH_4^+, which represents 61 ± 9% of total organic N (i.e., PN + DON + NH_4^+). Such a large accumulation of DON + NH_4^+ requires an imbalance between DON + NH_4^+ production and consumption, at least initially [e.g., *Thomas et al.*, 2001]. Sea ice efficiently traps living and

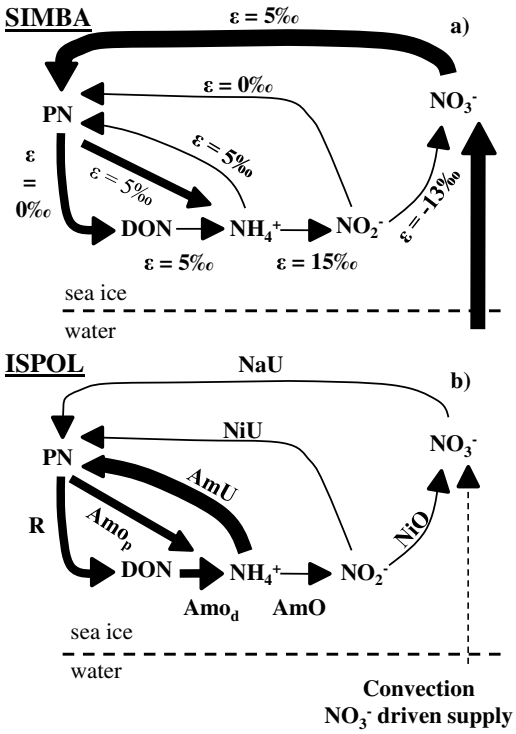

Figure 6. Schematic view of the internal N cycle with the associated isotope effects for each transformation process, for (a) SIMBA and (b) ISPOL. NaU indicates nitrate assimilation (U for uptake), *R* is DON release, Amo is ammonification (with the subscript *p* for PN → NH_4^+ and *d* for DON → NH_4^+), AmO is ammonium oxidation, AmU is ammonium assimilation, NiO is nitrite oxidation, and NiU is nitrite assimilation [after *DiFiore et al.*, 2009]. The arrow line thickness indicates the relative magnitude of the flux. SIMBA isotopic compositions are mainly inherited from previous nitrate assimilation and the concomitant large imbalance between DON + NH_4^+ production and consumption. For ISPOL, we suggest that this initial imbalance is attenuated with time via the development of an efficient regeneration loop (and thus a balance between DON + NH_4^+ production and consumption). For ISPOL, we assume that little nitrate is supplied from seawater because the salinity of the brine is lower than the salinity of seawater, thereby preventing brine overturning [*Tison et al.*, 2008].

decaying organic matter within the tortuosity of the brine network, and the organic matter is further embedded in a gel-like exopolymeric substance [*Deming*, 2010]. Given the strong seasonality of sea ice primary production, a seasonal delay between primary production and the development of an efficient heterotrophic community would not be surprising, and it can explain the imbalance between DON + NH_4^+ production and consumption (Figure 6a).

Field and laboratory studies suggest that both bacteria and zooplankton preferentially degrade low-δ^{15}N PN to ammonium, with a net isotope effect of ~2–5‰ [e.g., *Knapp et al.*, 2011; *Möbius*, 2013, and references therein]. Ammonification (DON, PN → NH_4^+) is likely the main discriminating step in this remineralization process. The release of DON from PN (PN → DON) will only occasionally involve the breaking of N-containing bonds, and the isotopic fractionation associated with bond breakage will be diluted across all the N atoms in the newly produced DON molecule; therefore, weaker isotopic fractionation is expected in DON release than in ammonification [*Knapp et al.*, 2011].

In the case (a) that PN is the ultimate end product of nitrate assimilation, PN δ^{15}N should be characterized by the accumulated product solution (equation (3)).

In an alternative case (b) of highly efficient conversion of PN to DON + NH_4^+ with no isotopic fractionation, PN should follow the instantaneous product equation (equation (2)), while DON + NH_4^+ (if the ultimate end product) should resemble the accumulated product.

In the case (c) of highly efficient conversion of PN to DON + NH_4^+ and significant isotopic fractionation during PN degradation to DON + NH_4^+, PN δ^{15}N may fall "above" the instantaneous product solution, and DON + NH_4^+ δ^{15}N may fall "below" the accumulated product solution. In all of the above cases, total reduced N (PN + DON + NH_4^+) should follow the accumulated product.

We have attempted to plot the SIMBA PN, DON + NH_4^+, and total reduced N data in Rayleigh space (data markers in Figure 5a), although the *x* axis (fraction of NO_3^- remaining) is potentially compromised by regenerated sources of nitrate as well as exchange with the underlying sea water. In general, the data are consistent with the efficient shunting of PN to DON + NH_4^+ (cases b or c). That PN δ^{15}N is higher in some cases than either of the instantaneous product curves while DON + NH_4^+ is lower in some cases than the accumulated product curves appears to favor the occurrence of isotope fractionation during the degradation of PN to DON + NH_4^+ (case c).

The ISPOL data indicate a lower $\Delta^{15}N_{PN-DON}$ (= $\delta^{15}N_{PN} - \delta^{15}N_{DON + NH4}$) than at SIMBA (i.e., the δ^{15}N of DON + NH_4^+ was higher and the δ^{15}N of PN was lower; Figures 2d and 5b). Occurring later in the growing season and consistent with the decaying stage of sea ice [*Tison et al.*, 2008], a more efficient coupling between DON + NH_4^+ production and consumption likely accounts for the observed similarity between PN

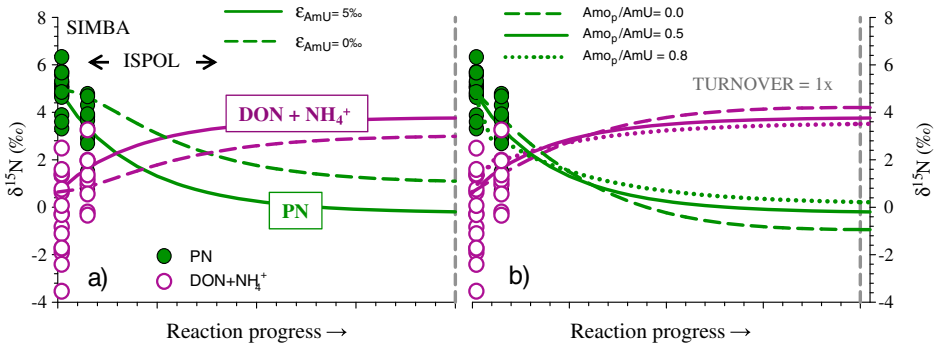

Figure 7. Observations (circles) and model (lines) taking into account an ideal regeneration loop (PN, DON → NH_4^+ → PN) and describing the δ^{15}N evolution of PN (green) and DON + NH_4^+ (purple), taking SIMBA δ^{15}N as initial conditions (i.e., before the development of a strong regeneration loop). (a) The simulation with an Amo_p/AmU ratio of 0.5 (Amo_p being PN → NH_4^+ and AmU being NH_4^+ → PN), no isotope fractionation for DON release (PON → DON), an isotope effect of 5‰ for ammonification (PN, DON → DON), and an isotope effect of 0 (dashed lines) and 5‰ (full lines) for ammonium assimilation (NH_4^+ → PN). (b) The simulations with no isotope fractionation for DON production, an isotope effect of 5‰ for both ammonium assimilation and ammonification, and an Amo_p/AmU ratio of 0.0 (dashed line), 0.5 (full line), and 0.8 (dotted line). Consistent with the observations, the pool sizes are 15 μmol l^{-1} for PN, 30 μmol l^{-1} for DON, and 5 μmol l^{-1} for ammonium. One complete turnover of the DON pool is indicated by the gray dashed line.

and DON + NH_4^+ δ^{15}N at ISPOL (Figure 5b). For an "ideal" regeneration loop (PN, DON → NH_4^+ → PN) in steady state, the mass balance implies (Figure 6):

$$\mathrm{AmU} = R + \mathrm{Amo}_p = \mathrm{Amo}_d + \mathrm{Amo}_p \tag{5}$$

in which: AmU is the rate of ammonium uptake, R is the rate of DON production, and Amo is the rate of ammonification (the subscript p is for PN → NH_4^+ and d for DON → NH_4^+; Figure 6), with the reasonable hypothesis that fractionation is identical for deamination of PN and DON ($\varepsilon_{\mathrm{Amop}} = \varepsilon_{\mathrm{Amod}}$). We can solve the isotopic balance for DON:

$$R \cdot \delta^{15}\mathrm{N}_R = \mathrm{Amo}_d \cdot \delta^{15}\mathrm{N}_{\mathrm{Amod}} \tag{6}$$

Since $R = \mathrm{Amo}_d$, it follows that $\delta^{15}\mathrm{N}_R = \delta^{15}\mathrm{N}_{\mathrm{Amod}}$, and since $\delta^{15}\mathrm{N}_R = \delta^{15}\mathrm{N}_{\mathrm{PN}} - \varepsilon_R$ and $\delta^{15}\mathrm{N}_{\mathrm{Amod}} = \delta^{15}\mathrm{N}_{\mathrm{DON}} - \varepsilon_{\mathrm{Amo}}$, we can rearrange equation (6) as

$$\delta^{15}\mathrm{N}_{\mathrm{PN}} = \delta^{15}\mathrm{N}_{\mathrm{DON}} + \varepsilon_R - \varepsilon_{\mathrm{Amo}} \tag{7}$$

Also, considering the isotopic balance for the PN pool, and since $\delta^{15}\mathrm{N}_{\mathrm{AmU}} = \delta^{15}\mathrm{N}_{\mathrm{NH4}} - \varepsilon_{\mathrm{AmU}}$, one derives that

$$\delta^{15}\mathrm{N}_{\mathrm{NH4}} = \delta^{15}\mathrm{N}_{\mathrm{PN}} + g \cdot (\varepsilon_R - \varepsilon_{\mathrm{Amo}}) - \varepsilon_R + \varepsilon_{\mathrm{AmU}} \tag{8}$$

where $g = \mathrm{Amo}_p/\mathrm{AmU} = 1 - (\mathrm{Amo}_d/\mathrm{AmU}) = 1 - (R/\mathrm{AmU})$. Comparing equations (7) and (8), the δ^{15}N convergence of PN and DON + NH_4 might be taken as an indication that ε_R is of similar magnitude to $\varepsilon_{\mathrm{Amo}}$. However, as discussed above, the expectation based on previous work is that ε_R is smaller than $\varepsilon_{\mathrm{Amo}}$ [e.g., *Knapp et al.*, 2011]. One explanation for this apparent discrepancy is that ISPOL has not reached steady state with regard to the PN, DON → NH_4^+ → PN regeneration loop. We can simulate how the initial $\Delta^{15}\mathrm{N}_{\mathrm{PN\text{-}DON}}$ at SIMBA, inherited from the near-complete nitrate depletion and concomitant DON + NH_4^+ imbalance, should have evolved in the development of an ideal regenerated loop (Figure 7). If it is assumed that the first step of remineralization (PN → DON) discriminates less than the second step (PN, DON → NH_4^+) [*Knapp et al.*, 2011], with time, DON + NH_4^+ and PN δ^{15}N should converge, and then the δ^{15}N of DON + NH_4^+ should become greater than that of PN δ^{15}N (Figure 7), as is observed in the subtropical surface waters [*Knapp et al.*, 2011]. Since, for both SIMBA and ISPOL, the δ^{15}N of DON + NH_4^+ was lower than that of PN, the implication is that the regeneration loop has not reached steady state (from Figures 4b and 4c to 6a and 6b).

5.3. Biologically Driven Sea Ice Nitrate Regeneration: Nitrification

The difference between measured NO_3^- δ^{15}N and that expected from Rayleigh fractionation (equation (1)), as well as the simple observation of nitrate with a δ^{15}N lower than that in the underlying seawater, point to nitrification along with nitrate assimilation as a key control on the distribution of the nitrate isotopes.

In this section, we will (i) consider how nitrification could affect the $\delta^{15}N$ of fixed N and (ii) use mass and isotopic balances to estimate the ratio of nitrification to nitrate assimilation.

Previous evidence for nitrification in sea ice exists, mainly in landfast sea ice. *Priscu et al*. [1990] measured the first step of nitrification, the oxidation of NH_4^+ to NO_2^-, using ^{13}C incubations with an inhibitor of NH_4^+ oxidizing bacteria. Additional evidence comes from the studies documenting accumulation of both nitrite and nitrate [*Arrigo et al*., 1995; *Riaux-Gobin et al*., 2000; *Cozzi*, 2008] and the accumulation of phaeopigments, ammonium, and nitrite in sea ice [*Riaux-Gobin et al*., 2005]. Nitrifiers tend to grow in aggregate, excrete exopolymeric substances, and embed in biofilms [*Hagopian and Riley*, 1998]. In sea ice, high concentrations of exopolymeric substance have been measured, and the microbial community is indeed embedded in a biofilm [*Meiners et al*., 2004; *Deming*, 2010]. With its potentially large source of ammonium (from remineralization of PN and DON), sea ice thus appears to be a favorable environment for nitrification.

Nitrification occurs in two steps (Figure 6), the oxidation of ammonium to nitrite and the oxidation of nitrite to nitrate, mediated by distinct groups of microorganisms. Ammonium that is produced by ammonification may be reassimilated by algae or oxidized to NO_2^-. Nitrite itself can then be assimilated or further oxidized to NO_3^-. The ratio of these two processes—assimilation and oxidation—and their associated isotope effects will affect the $\delta^{15}N$ of both reactants and products.

A large and variable isotope effect has been estimated for NH_4^+ assimilation (AmU), from ~5 to ~22‰ [*Vo et al*., 2013]. Its expressed magnitude appears to be dependent on the external ammonia (NH_3) concentration, which controls active versus passive ammonium/ammonia diffusion across the cell membrane. NH_3 concentration is dependent on the equilibrium constants, NH_4^+ concentration, and pH [*Bange*, 2007]. The average brine pH for SIMBA and ISPOL was 8.5 ± 0.3 (B. Delille, unpublished result, 2013). Using a pK_a of ~10.0 for seawater at 0°C, the NH_3 concentration should be below 0.1 $\mu mol\, l^{-1}$ for both ISPOL and SIMBA. At such concentrations, an AmU isotope effect of ~5‰ has been observed, the magnitude of which is set by the rate-limiting step of active NH_4^+ transport and the subsequent passive transport of NH_3 back into the external medium [*Vo et al*., 2013]. Ammonium oxidation (AmO) by marine nitrifiers strongly fractionates the N isotopes, with an isotope effect between 12 and 19‰ [*Casciotti et al*., 2003]. A low isotope effect for nitrite assimilation (NiU) has been measured (less than 1‰) [*Waser et al*., 1998]. Nitrite oxidation (NiO) has the rare characteristic of having an inverse isotope effect, with ^{15}N nitrite being preferentially oxidized (−13‰) [*Casciotti*, 2009]. For the following, we assume an isotope effect of 5‰ for ammonium assimilation, 15‰ for ammonium oxidation, 0‰ for nitrite assimilation, and −13‰ for nitrite oxidation (Figure 6).

Given the discussion above, the main processes acting on the regenerated NO_3^- $\delta^{15}N$ are production and consumption of NH_4^+ and the oxidation of NO_2^-. For both SIMBA and ISPOL, organic N was by far the dominant N form, introducing considerable inertia to the internal cycling of N. This organic N should impose its relatively constant isotopic composition, mainly inherited from previous organic N production (see section 5.2), on its release of N (i.e., ammonification; Amo) for both NH_4^+ assimilation (AmU) and oxidation (i.e., nitrification; AmO). The $\delta^{15}N$ of ammonium and its products (PN, NO_2^-,and NO_3^-) will depend on the combination of isotope effects, the relative importance of which are weighted by their relative contribution to NH_4^+ and NO_2^- removal, as follows (where *x* and *y* are AmU/Amo and NiU/AmO, respectively; Figure 8):

$$\delta^{15}{}_{NH_4^+} = \delta^{15}N_{PN,DON} - \varepsilon_{Amo} + x \cdot (\varepsilon_{AmU} - \varepsilon_{AmO}) + \varepsilon_{AmO} \quad (9)$$

$$\delta^{15}{}_{PN\text{-regenerated}} = \delta^{15}N_{PN,DON} - \varepsilon_{Amo} + x \cdot (\varepsilon_{AmU} - \varepsilon_{AmO}) + \varepsilon_{AmO} - \varepsilon_{AmU} \quad (10)$$

$$\delta^{15}{}_{NO_3^- - regenerated} = \delta^{15}N_{PN,DON} - \varepsilon_{Amo} + x \cdot (\varepsilon_{AmU} - \varepsilon_{AmO}) + y \cdot (\varepsilon_{NiU} - \varepsilon_{NiO}) \quad (11)$$

where $\delta^{15}N_{PN,\,DON}$ is the weighted average of PN and DON + NH_4^+ $\delta^{15}N$ for both ISPOL and SIMBA. The equations above predict that varying *x* and *y* from 0 to 1 yields regenerated nitrate with a $\delta^{15}N$ between 10 and −13‰ (Figure 8). Considering the lower half of this range, a contribution from nitrification can explain the low $\delta^{15}N$ that we observe for sea ice nitrate (Figures 2b and 2d).

It seems unlikely that a larger fraction of the ammonium produced by ammonification (PN, DON → NH_4^+) will be oxidized rather than assimilated. The energy yield of ammonium oxidation is low [*Hagopian and Riley*, 1998; *Ward*, 2007], and nitrifiers should not be able to out-compete sea ice algae for the available stock of

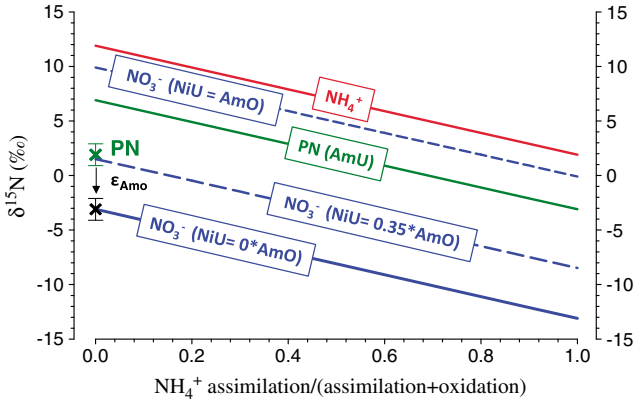

Figure 8. Steady state model describing the δ^{15}N of both reactants and products (PN, DON → NH_4^+ → NO_2^- → NO_3^-) as a function of the NH_4^+ assimilation/(oxidation + assimilation) ratio (AmU/AmO + AmU), assuming a constant source for regenerated N (black cross with error bar on the left), i.e., organic N (green cross with error bar; weighted average for both SIMBA and ISPOL) minus the isotope effect for ammonification (Amo). Regenerated NO_3^- δ^{15}N also depends on the NO_2^- assimilation/(oxidation + assimilation) ratio (equation (11), NiU/NiO + NiU), with two end-members: NiU = AmO (nitrite uptake = ammonium oxidation; small dashed blue line) and NiO = AmO (nitrite oxidation = ammonium oxidation; solid blue line). The medium dashed line is for a NO_2^- assimilation/(oxidation + assimilation) ratio of 0.35 (see section 5.3) [*Olson*, 1981]. The acronyms are described in Figure 6.

ammonium, unless they are able take advantage of low light periods. Accordingly, if the NH_4^+ assimilation/(oxidation + assimilation) ratio (x in equation (11) and x axis in Figure 8) is greater than 0.5 [e.g., *Olson*, 1981; *Bianchi et al*., 1997], regenerated nitrate δ^{15}N should range between 5 and −13‰. To our knowledge, *Olson* [1981] is the only study reporting the contribution of NO_2^- assimilation to the NO_2^- removal (y ratio in equation (11)), with a maximum contribution of 0.35 in the Southern Ocean. By varying the x (x axis in Figure 8) and y ratios from 0.5 to 1 and 0 to 0.35, respectively, regenerated nitrate δ^{15}N should fall between −3.5 and −13‰ (Figure 8).

Assuming a closed system following a convective event (section 5.1), and both nitrate assimilation and nitrification as the main processes acting on the nitrate pool, we solve the mass and isotopic balances for each depth (weighted averages in Figures 2b and 2d) to estimate the contribution of nitrification to nitrate assimilation (see supporting information, section 4, for a more detailed description of the model and the optimization scheme). With no significant depth variation and no major difference between SIMBA and ISPOL, satisfying solutions (i.e., within the analytical error bars for nitrate concentration and δ^{15}N; Figures S7a and S7b) are found if nitrification contributes between 29 ± 2 and 66 ± 8% to nitrate assimilation. This range of values results from varying the δ^{15}N of regenerated nitrate from −13 to −3.5‰, respectively (Figure 8). The only exception is for the bottom community at ISPOL, where satisfying solutions are found with a smaller contribution of nitrification to NO_3^- assimilation (3 to 30%). This is perhaps to be expected, given the relative ease with which the bottom community can interact with seawater nitrate. Our analysis implies that within Antarctic sea ice during early spring to early summer, nitrate behaves as a regenerated nutrient. This finding has significant implications for our understanding and parameterization of sea ice N cycling; current sea ice biogeochemical models typically assume little or no NO_3^- regeneration [e.g., *Tedesco et al*., 2012].

Our parameterization (with zero-order reactions) does not take into account the temporal decoupling between primary production and the development of a fully efficient microbial loop, including nitrifiers. Once the nitrate is consumed to low concentration, subsequent nitrification should have a greater impact on the δ^{15}N of nitrate than in the context of a steady state between nitrate assimilation and nitrification. Another source of uncertainty is that NO_2^- can be also produced by autotrophic cells, from an imbalance between NO_3^- and NO_2^- reduction during NO_3^- assimilation and the following NO_2^- efflux out of the cells [*Olson*, 1981] (median contribution to NO_2^- production = 0.1). The isotope effect associated with NO_3^- assimilation is thought to occur primary with the rate-limiting NO_3^- reductive step into NO_2^- [*Granger et al*., 2004]. The NO_2^- efflux δ^{15}N out of the cell should be therefore similar to PN (equation (2) and Figures 2b and 2d). Such contribution should increase the NO_2^- δ^{15}N by 0.5 and 1.5‰ for a regenerated NO_3^- δ^{15}N of −3.5 and −13‰, respectively (Figure 8). Clearly, further work is required to better constrain the N mass and isotopic balances in sea ice. Nitrate δ^{18}O measurements should provide further insights into nitrate regeneration [*DiFiore et al*., 2009], and measurements of ammonium and nitrite δ^{15}N will allow us to disentangle the ammonium-/nitrite-associated processes, improving our estimates of regenerated nitrate δ^{15}N (e.g., Figure 8).

5.4. Paleoceanographic Implications

The only study reporting N isotope distributions in Antarctic sea ice observed a δ^{15}N for PN that was significantly higher than the δ^{15}N of water column PN, 2 to 41‰ versus −6 to 6‰, respectively [*Rau et al*., 1991;

DiFiore et al., 2009]. *Rau et al*. [1991] suggested that volatization (i.e., the loss of N as ammonia), followed by ammonium assimilation, was the mechanism leading to the highest δ^{15}N of sea ice PN. During the last ice age, the δ^{15}N of diatom-bound organic N in Antarctic sediments was 0 to 10‰ higher than it is today [*Robinson and Sigman*, 2008], which has been interpreted as evidence of enhanced nutrient consumption. This explanation assumes, among other things, that diatom production and sinking biogenic matter derived predominantly from the water column. During the ice ages, the extent of sea ice cover likely expanded equatorward [*Gersonde et al*., 2005]. Using the highest δ^{15}N measured in sea ice PN δ^{15}N by *Rau et al*. [1991], 41‰, we calculate that a ~5% increase in the contribution of sea ice to sedimentary organic N would induce a shift of ~3‰ in its δ^{15}N. This calculation also roughly applies to diatom-bound N, as much of the phytoplankton growth in sea ice is by diatoms. This calculation makes the simple point that if sea ice PN δ^{15}N can be very high, then trivial changes in its contribution to Antarctic sediments could relatively easily explain the observed glacial/interglacial δ^{15}N change.

We have shown that sea ice PN δ^{15}N is set by partial nitrate consumption, nitrate resupply through brine convection, and the balance between DON production and consumption. Given the preferential assimilation of ^{14}N by phytoplankton, the δ^{15}N of both nitrate and organic N increases when the nitrate pool is progressively depleted during the sea ice algal bloom. Assuming a nitrate source at 5‰ and an isotope effect for nitrate assimilation of 5‰ [*Difiore et al*., 2009; *Rafter et al*., 2013], organic N (i.e., the accumulated product; equation (3)) should range from 0 to 5‰ for zero and complete nitrate consumption, respectively. The efficient shunting of PN to DON + NH_4^+ at the beginning of the sea ice algal bloom implies that PN δ^{15}N is initially better characterized by the instantaneous product (equation (2)), representing newly formed biomass, and can thus be higher (by a few permil) than the accumulated product (see section 5.2). The imbalance between DON + NH_4^+ production and consumption is attenuated with time due to the impact of regenerated primary production. This promotes the convergence of PN δ^{15}N on the δ^{15}N of the total organic N pool (PN + DON + NH_4^+), i.e., the accumulated product (equation (3); from 0 to 5‰; see section 5.2).

Such behavior of sea ice PN δ^{15}N is similar to that of PN in the euphotic layer of the open ocean, which is driven by nitrate assimilation and wintertime nitrate supply [*Sigman et al*., 1999]. Since the degree of nitrate consumption (equation (4)) is greater in sea ice than in the present day Antarctic Zone, sea ice PN δ^{15}N (−0.9 to 6.3‰, median = 4.5‰, n = 141) is significantly higher than the δ^{15}N of PN in seawater (−6 to 6‰, average = 0.6‰) [*Rau et al*., 1991; *DiFiore et al*., 2009]. However, we did not observe the much higher PN δ^{15}N as occasionally measured by *Rau et al*. [1991]. Ammonia volatization, as suggested by *Rau et al*. [1991], would preferentially expel ^{14}N from the sea ice, increasing the δ^{15}N of sea ice TN, which is the opposite of what we observe (Figure 3). Such occasional high values are theoretically achievable by the instantaneous product under near-complete nitrate consumption (equation (2)), but with no concomitant regeneration since even a small amount of ammonium assimilation will drive the δ^{15}N of the PN back toward the δ^{15}N of the accumulated product (equation (3)). Arctic studies have shown an overlap between sea ice and seawater PN δ^{15}N (3.9 to 13.5‰ versus 0.0 to 12.6‰, respectively) [*Tamelander et al*., 2008; *Gradinger*, 2009; *Pineault et al*., 2013], with only one study reporting higher PN δ^{15}N in sea ice (8.3‰) than in seawater (4.9‰) [*Hobson et al*., 1995]. The surface waters of the open Arctic are lower [NO_3^-] (<5 μmol l^{-1}) relative to the Antarctic (~ 30 μmol l^{-1}). Such near-complete NO_3^- depletion in both the Arctic mixed layer and the sea ice is expected and largely observed to yield similar PN δ^{15}N in these two Arctic environments of algal growth (equation (3)).

From the analysis above, it seems unlikely that sea ice alone can explain the variations in sedimentary PN δ^{15}N during the last ice age [*Robinson and Sigman*, 2008]. Indeed, sea ice PN is only ~3–4‰ higher in δ^{15}N than its marine counterpart, requiring that sea ice came to dominate sedimentary PN (and diatom-bound N) if it were to explain most of the glacial/interglacial signal. Today, net organic N production (i.e., given by nitrate depletion) in sea ice represents only a few percent in the seasonal ice zone and in the permanently open ocean zone of the Antarctic [e.g., *Arrigo and Thomas*, 2004], such that it is unlikely that sea ice was ever the sole source of organic N to the sediments of these zones. However, given the dramatic decrease in Antarctic productivity during the last ice age [*Kohfeld et al*., 2005] and the concomitant equatorward sea ice expansion [*Gersonde et al*., 2005], we cannot rule out a role for sea ice production in the δ^{15}N variations in sediment cores closer to the Antarctic continent. Under conditions of more permanent sea ice cover, the sea ice contribution to sedimentary organic N should increase. Indeed, the two southernmost sediment cores in the compilation of *Robinson and Sigman* [2008] are located close to the modern extent of winter sea ice, and these show the

largest $\delta^{15}N$ variation across glacial-interglacial cycles [*Robinson and Sigman*, 2008]. Further work should focus on investigating the $\delta^{15}N$ of diatom-bound N produced within Antarctic sea ice.

6. Conclusions

We report nitrate, total dissolved nitrogen, and particulate nitrogen isotope data from the Antarctic pack ice in the Weddell Sea (ISPOL, December 2004) and the Bellinghausen Sea (SIMBA, October 2007). The objectives were twofold: (i) to use the isotopic distributions to better constrain biogeochemical dynamics and (ii) to provide robust information with which to assess the impact on the N isotopic composition of the organic matter in Antarctic sediments and sedimentary fractions. Within the sea ice collected during two sampling campaigns, the nitrate concentration was significantly depleted relative to the underlying seawater. The accumulation of organic N (the dominant form of fixed N) clearly suggested that the in situ microbial community and biogeochemical conditions were mainly inherited from an earlier period of NO_3^- assimilation.

The $\delta^{15}N$ of sea ice total nitrogen (PN + TDN) was significantly lower than that of NO_3^- (and thus the TN) of the underlying seawater. This difference implies the preferential loss of ^{15}N during the growth and decay of sea ice. We suggest that the coupling of nitrate assimilation, which traps ^{14}N into biomass within the sea ice, with brine convection is a viable mechanism to explain the low-$\delta^{15}N$ TN across the ice floe. In general, nitrate $\delta^{15}N$ in the sea ice was lower than in underlying seawater. Nitrification is the only viable mechanism that explains this observation, as it supplies low-$\delta^{15}N$ regenerated nitrate. In a first effort to quantify the relative importance of this process, nitrification was found to contribute substantially (up to ~70%) to the nitrate being assimilated within the ice. The $\delta^{15}N$ of total organic N (PN + DON + NH_4^+) was similar to expectations for NO_3^- assimilation in a closed environment (i.e., the accumulated product of Rayleigh fractionation). However, the $\delta^{15}N$ differed amongst the different organic N forms, with the $\delta^{15}N$ of DON + NH_4^+ being lower than PN $\delta^{15}N$. Together with the large accumulation of DON + NH_4^+, this suggests an imbalance between DON + NH_4^+ production and consumption. We suggest that DON + NH_4^+ represents the end product of earlier nitrate assimilation into PN, which preferentially accumulated ^{14}N and then passed its low $\delta^{15}N$ on to DON + NH_4^+, with isotopic fractionation in the conversion. The $\delta^{15}N$ elevation of PN relative to DON + NH_4^+ occurred to a lesser extent at ISPOL (~1.7‰) relative to SIMBA (~5.7‰). Conditions at ISPOL were characteristic of the decaying stage of sea ice [*Tison et al*., 2008] such that an efficient regeneration loop (PN, DON → NH_4^+ → PN) following the main peak in productivity was being established, driving the $\delta^{15}N$ of PN to converge on that of the DON + NH_4^+.

We conclude that nitrate assimilation resulting in the net production of low-$\delta^{15}N$ organic N is a dynamic common to both the water column and the sea ice of the Antarctic, although nitrate assimilation is more complete within the ice. Thus, the contribution of sea ice organic N to sedimentary $\delta^{15}N$ should be less distinct from (only a few permil higher than) that of the water column than has been proposed previously [*Rau et al*., 1991]. This makes it correspondingly more difficult for sea ice to explain the higher $\delta^{15}N$ of Antarctic sediments and diatom-bound N during the last ice age (0 to 10‰ higher than Holocene). To do so, sea ice-internal organic matter would need to have been the dominant source of sedimentary and diatom-bound N during the last ice age.

Acknowledgments

Our warm thanks go to the officers and crews of the RVIB *Nathaniel B. Palmer* (SIMBA) and RV *Polarstern* (ISPOL), as well to the chief scientists, respectively, C. Haas and S. Ackley. We are also grateful to S. Oleynik for the management of the GC/IRMS laboratory at Princeton University; to S. El Amri (ULB) for her help in sample processing. This research was supported by the Communauté Française de Belgique (SIBClim project, ARC contract 02/07-287), the Belgian Science policy (BIGSOUTH network, SD/CA/05A of SPSDIII, Support Plan for Sustainable Development), the U.S. NSF through grant OPP-0453680, and by the Grand Challenges Program at Princeton University. François Fripiat was and is a postdoctoral fellow with the "Fonds National de la Recherche Scientifique" (FNRS, Belgium) and "Fonds Wetenschappelijk Onderzoek" (FWO, Belgium), respectively.

References

Altabet, M. A., and R. François (1994), Sedimentary nitrogen isotopic ratio as a recorder for surface ocean nitrate utilization, *Global Biogeochem. Cycles*, *8*(1), 103–116.

Arrigo, K. R., and D. N. Thomas (2004), Large scale importance of sea ice biology in the Southern Ocean, *Antarctic Sci.*, *16*(4), 471–486.

Arrigo, K. R., G. Dieckmann, M. Gosselin, D. H. Robinson, C. H. Fritsen, and C. W. Sullivan (1995), High resolution study of the platelet ice ecosystem in McMurdo Sound, Antarctica: Biomass, nutrient, and production profiles within a dense microbial bloom, *Mar. Ecol. Prog. Ser.*, *127*, 255–268.

Bange, H. W. (2007), Gaseous nitrogen compounds (NO, N_2O, N_2, NH_3) in the ocean, in *Nitrogen in the Marine Environment*, edited by D. G. Capone et al., Elsevier, Amsterdam, Netherlands.

Bianchi, M., F. Feliatra, P. Tréguer, M.-A. Vincendeau, and J. Morvan (1997), Nitrification rates, ammonium and nitrate distribution in upper layers of the water column and in sediments of the Indian sector of the Southern Ocean, *Deep Sea Res., Part II*, *44*(5), 1017–1032.

Böhlke, J. K., S. J. Mroczkowkski, and T. B. Coplen (2003), Oxygen isotope in nitrate: New reference materials for ^{18}O:^{17}O:^{16}O measurements and observations on nitrate-water equilibration, *Rapid Commun. Mass Spectrom.*, *17*, 1835–1846.

Braman, R. S., and S. A. Hendrix (1989), Nanogram nitrite and nitrate determination in environmental and biological materials by vanadium (III) reduction with chemiluminescence detection, *Anal. Chem.*, *61*, 2715–2718.

Casciotti, K. L. (2009), Inverse kinetic isotope fractionation during bacterial nitrite oxidation, *Geochim. Cosmochim. Acta*, *73*, 2061–2076.

Casciotti, K. L., D. M. Sigman, and B. B. Ward (2003), Linking diversity and stable isotope fractionation in ammonia-oxidizing bacteria, *Geomicrobiol. J.*, *20*, 335–353.

Cox, G. F. N., and W. F. Weeks (1983), Equations for determining the gas and brine volumes in sea-ice samples, *J. Glaciol.*, *29*(102), 306–316.
Cozzi, S. (2008), High-resolution trends of nutrients, DOM and nitrogen uptake in the annual sea ice at Terra Nova Bay, Ross Sea, *Antarct. Sci.*, *20*(5), 441–454.
Deming, J. W. (2010), Sea ice bacteria and viruses, in *Sea Ice*, edited by D. N. Thomas and G. S. Dieckmann, Blackwell Science, Ltd., Oxford, U. K.
Difiore, P. J., D. M. Sigman, and R. B. Dunbar (2009), Upper ocean nitrogen fluxes in the Polar Antarctic Zone: Constraints from the oxygen and nitrogen isotopes of nitrate, *Geochem. Geophys. Geosyst.*, *10*, Q11016, doi:10.1029/2009GC002468.
Difiore, P. J., D. M. Sigman, K. L. Karsh, T. W. Trull, R. B. Dunbar, and R. S. Robinson (2010), Poleward decrease in the isotope effect of nitrate assimilation across the Southern Ocean, *Geophys. Res. Lett.*, *37*, L17601, doi:10.1029/2010GL044090.
François, R., M. A. Altabet, E. F. Yu, D. M. Sigman, M. P. Bacon, M. Frank, G. Bohrmann, G. Bareille, and L. D. Labeyrie (1997), Contribution of Southern Ocean surface-water stratification to low atmospheric CO_2 concentration during the last glacial period, *Nature*, *389*, 929–935.
Fripiat, F., D. Cardinal, J.-L. Tison, A. Worby, and L. André (2007), Diatom-induced silicon isotopic fractionation in Antarctic sea ice, *J. Geophys. Res.*, *112*, G02001, doi:10.1029/2006JG000244.
Garside, C. (1982), A chemiluminescent technique for the determination of nanomolar concentrations of nitrate and nitrite in seawater, *Mar. Chem.*, *11*, 159–167.
Gersonde, R., X. Crosta, A. Abelmann, and L. Armand (2005), Sea-surface temperature and sea ice distribution of the Southern Ocean at the EPILOG Last Glacial Maximum—A circum-Antarctic view based on siliceous microfossil records, *Quaternary Sci. Rev.*, *24*, 869–896.
Gleitz, M., M. R. van der Loeff, D. N. Thomas, G. S. Dieckmann, and F. J. Millero (1995), Comparison of summer and winter inorganic carbon, oxygen and nutrient concentrations in Antarctic sea ice brine, *Mar. Chem.*, *51*, 81–91.
Golden, K. M., S. F. Ackley, and V. I. Lytle (1998), The percolation phase transition in sea ice, *Science*, *282*, 2238–2241.
Gosselin, M., M. Levasseur, P. A. Wheeler, R. A. Horner, and B. C. Booth (1997), New measurements of phytoplankton and ice algal production in the Arctic Ocean, *Deep Sea Res., Part II*, *44*(8), 1623–1644.
Gradinger, R. (2009), Sea-ice algae: Major contributors to primary production and algal biomass in the Chukchi and Beaufort Seas during May/June 2002, *Deep Sea Res., Part II*, *56*, 1201–1212.
Granger, J., D. M. Sigman, J. A. Needoba, and P. J. Harrison (2004), Coupled nitrogen and oxygen isotope fractionation of nitrate during assimilation by cultures of marine phytoplankton, *Limnol. Oceanogr.*, *49*(5), 1763–1773.
Granger, J., and D. M. Sigman (2009), Removal of nitrite with sulfamic acid for nitrate N and O isotope analysis with the denitrifier method, *Rapid Commun. Mass Spectrom.*, *23*, 3753–3762.
Griewank, P. J., and D. Notz (2013), Insights into brine dynamics and sea ice desalination from a 1-D model study of gravity drainage, *J. Geophys. Res. Oceans*, *118*, 3370–3386, doi:10.1002/jgrc.20247.
Hagopian, D. S., and J. G. Riley (1998), A closer look at the bacteriology of nitrification, *Aquacult. Eng.*, *19*, 223–244.
Hobson, K. A., W. G. Ambrose Jr., and P. E. Renaud (1995), Sources of primary production, benthic-pelagic coupling, and trophic relationships within the Northeast Water Polynya: Insights from δ13C and δ15N analysis, *Mar. Ecol. Prog. Ser.*, *128*, 1–10.
Holmes, R. M., A. Aminot, R. Kérouel, B. A. Hooker, and B. J. Peterson (1999), A simple and precise method for measuring ammonium and marine and freshwater ecosystems, *Can. Data Rep. Fish. Aquat. Sci.*, *56*, 1801–1808.
Jardon, F. P., F. Vivier, M. Vancoppenolle, A. Lourenço, P. Bouruet-Aubertot, and Y. Cuypers (2013), Full-depth desalination of warm sea ice, *J. Geophys. Res. Oceans*, *118*, 1–13, doi:10.1029/2012JC007962.
Knapp, A. N., D. M. Sigman, and F. Lipschultz (2005), N isotopic composition of dissolved organic nitrogen and nitrate at the Bermuda Atlantic Time-series Study site, *Global Biogeochem. Cycles*, *19*, GB1018, doi:10.1029/2004GB002320.
Knapp, A. N., D. M. Sigman, F. Lipschultz, A. B. Kustka, and D. G. Capone (2011), Interbasin isotopic correspondence between upper-ocean bulk DON and subsurface nitrate and its implications for marine nitrogen cycling, *Global Biogeochem. Cycles*, *25*, GB4004, doi:10.1029/2010GB003878.
Kohfeld, K. E., C. Le Quéré, S. P. Harrison, and R. F. Anderson (2005), Role of marine biology in glacial-interglacial CO_2 cycles, *Science*, *308*, 74–78.
Lannuzel, D., V. Schoemann, J. T. M. de Jong, L. Chou, B. Delille, S. Becquevort, and J.-L. Tison (2008), Iron study during a time series in the western Weddell pack ice, *Mar. Chem.*, *108*(1), 85–95.
Legendre, L., S. F. Ackley, G. S. Dieckmann, B. Gulliksen, R. Horner, T. Hoshiai, I. A. Melnikov, W. S. Reeburgh, M. Spindler, and C. W. Sullivan (1992), Ecology of sea ice biota, 2. Global significance, *Polar Biol.*, *12*, 429–444.
Lewis, M. J., J.-L. Tison, B. Weissling, B. Delille, S. F. Ackley, F. Brabant, and H. Xie (2011), Sea ice and snow cover characteristics during the winter-spring transition in the Bellingshausen Sea: An overview of SIMBA 2007, *Deep Sea Res., Part II*, *58*, 1019–1038.
Maksym, T., and T. Markus (2008), Antarctic sea ice thickness and snow-to-ice conversion from atmospheric reanalysis and passive microwave snow depth, *J. Geophys. Res.*, *113*, Q11016, doi:10.1029/2006JC004085.
McPhee, M. G. (2008), Physics of early summer ice/ocean exchanges in the western Weddell Sea during ISPOL, *Deep Sea Res.*, *55*, 1075–1097.
Meiners, K., R. Brinkmeyer, M. A. Granskog, and A. Lindfors (2004), Abundance, size distribution and bacterial colonization of exopolymer particles in Antarctic sea ice (Bellingshausen Sea), *Aquat. Microb. Ecol.*, *35*, 283–296.
Möbius, J. (2013), Isotope fractionation during nitrogen remineralization (ammonification): Implications for nitrogen isotope biogeochemistry, *Geochim. Cosmochim. Acta*, *105*, 422–432.
Müller, S., A. V. Vähätalo, C. Stedmon, M. A. Granskog, L. Norman, S. N. Aslam, G. J. C. Underwood, G. S. Dieckmann, and D. N. Thomas (2013), Selective incorporation of dissolved organic matter (DOM) during sea ice formation, *Mar. Chem.*, doi:10.1016/j.marchem.2013.06.008, in press.
Notz, D., and M. G. Worster (2009), Desalination processes of sea ice revisited, *J. Geophys. Res.*, *114*, C05006, doi:10.1029/2008JC004885.
Ogawa, H., R. Fukuda, and I. Koike (1999), Vertical distributions of dissolved organic carbon and nitrogen in the Southern Ocean, *Deep Sea Res., Part I*, *46*, 1809–1826.
Olson, R. J. (1981), ^{15}N tracer studies of the primary nitrite maximum, *J. Mar. Res.*, *39*(2), 203–238.
Pineault, S., J.-E. Tremblay, M. Gosselin, H. Thomas, and E. Shadwick (2013), The isotopic signature of particulate organic C and N in bottom ice: Key influencing factors and applications for tracing the fate of ice-algae in the Arctic Ocean, *J. Geophys. Res. Oceans*, *118*, 287–300, doi:10.1029/2012JC008331.
Priscu, J. C., M. T. Downes, L. R. Priscu, A. C. Palmisano, and C. W. Sullivan (1990), Dynamic of ammonium oxidizer activity and nitrous oxide (N_2O) within and beneath Antarctic sea ice, *Mar. Ecol. Prog. Ser.*, *62*, 37–46.
Qi, H., T. B. Coplen, H. Geilmann, W. A. Brand, and J. K. Böhlke (2003), Two new organic reference materials for δ^{13}C and δ^{15}N measurements and a new value for the δ^{13}C of NBS22 oil, *Rapid Commun. Mass Spectrom.*, *17*, 2483–2487.
Rafter, P. A., P. J. DiFiore, and D. M. Sigman (2013), Coupled nitrate nitrogen and oxygen isotopes and organic matter remineralization in the Southern and Pacific oceans, *J. Geophys. Res. Oceans*, *118*, 4781–4794, doi:10.1002/jgrc20316, in press.

Rau, G. H., C. W. Sullivan, and L. I. Gordon (1991), δ^{13}C and δ^{15}N variations in Weddell Sea particulate organic matter, *Mar. Chem.*, *35*, 355–369.
Riaux-Gobin, C., P. Tréguer, M. Poulin, and G. Vétion (2000), Nutrients, algal biomass and communities in land-fast ice and seawater off Adélie Land (Antarctica), *Antarct. Sci.*, *12*(2), 160–171.
Riaux-Gobin, C., P. Tréguer, G. S. Dieckmann, E. Maria, G. Vétion, and M. Poulin (2005), Land-fast ice off Adélie Land (Antarctica): Short-term variations in nutrients and chlorophyll just before ice break-up, *J. Mar. Syst.*, *55*, 235–248.
Robinson, R. S., and D. M. Sigman (2008), Nitrogen isotopic evidence for a poleward decrease in surface nitrate within the ice age Antarctic, *Quaternary Sci. rev.*, *27*, 1076–1090.
Rysgaard, S., R. N. Glud, M. K. Sejr, M. E. Blichner, and J. Stahl (2008), Denitrification activity and oxygen dynamics in Arctic sea ice, *Polar Biol.*, *31*, 527–537.
Sigman, D. M., M. A. Altabet, D. C. McCorkle, R. François, and G. Fischer (1999), The δ^{15}N of nitrate in the Southern Ocean: Consumption of nitrate in surface waters, *Global Biogeochem. Cycles*, *13*(4), 1149–1166.
Sigman, D. M., K. L. Casciotti, M. Andreani, C. Barford, M. Galanter, and J. K. Böhlke (2001), A bacterial method for the nitrogen isotopic analysis of nitrate in seawater and freshwater, *Anal. Chem.*, *73*, 4145–4153.
Tamelander, T., M. Reigstad, H. Hop, M. L. Carroll, and P. Wassmann (2008), Pelagic and sympagic contribution of organic matter to zooplankton and vertical export in the Barents Sea marginal ice zone, *Deep Sea Res., Part II*, *55*, 2330–2339.
Tedesco, L., M. Vichi, and D. N. Thomas (2012), Process studies on the ecological coupling between sea ice algae and phytoplankton, *Ecol. Model.*, *226*, 120–138.
Thomas, D. N., and G. S. Dieckmann (2002), Antarctic sea ice—A habitat for extremophiles, *Science*, *295*, 641–644.
Thomas, D. N., G. Kattner, R. Engbrodt, V. Giannelli, H. Kennedy, C. Hass, and G. S. Dieckmann (2001), Dissolved organic matter in Antarctic sea ice, *Ann. Glaciol.*, *33*, 297–303.
Thomas, D. N., S. Papadimitriou, and C. Michel (2010), Biogeochemistry of sea ice, in *Sea Ice*, edited by D. N. Thomas and G. S. Dieckmann, Blackwell Science, Ltd., Oxford, U. K.
Tison, J.-L., A. Worby, B. Delille, F. Brabant, S. Papadimitriou, D. Thomas, J. de Jong, D. Lannuzel, and C. Haas (2008), Temporal evolution of decaying summer first-year sea ice in the western Weddell Sea, Antarctica, *Deep Sea Res., Part II*, *55*, 975–987.
Verdugo, P., A. L. Alldredge, F. Azam, D. L. Kirchman, U. Passow, and P. H. Santschi (2004), The oceanic gel phase: A bridge in the DOM-POM continuum, *Mar. Chem.*, *92*, 67–85.
Vo, J., W. Inwood, J. M. Hayes, and S. Kustu (2013), Mechanism for nitrogen isotope fractionation during ammonium assimilation by Escherichia Coli K12, *Proc. Natl. Acad. Sci.*, *110*(21), 8696–8701.
Ward, B. B. (2007), Nitrification in marine systems, in *Nitrogen in the Marine Environment*, edited by D. G. Capone et al., Elsevier, Amsterdam, Netherlands.
Waser, N. A. D., P. J. Harrison, B. Nielsen, and S. E. Calvert (1998), Nitrogen isotope fractionation during the uptake and assimilation of nitrate, nitrite, ammonium, and urea by a marine diatom, *Limnol. Oceanogr.*, *43*(2), 215–224.